# SURFACE EMISSIVITY EFFECT ON THE OPERATING TEMPERATURE OF CONCENTRATION TRIPLE JUNCTION SOLAR CELL

Fahad Al-Amri
College of Technology
PO Box: 7650; Dammam
31472; Saudi Arabia
e-mail:falamri1@tvtc.gov.sa

Tapas Kumar Mallick
Mechanical
Environment,
University of Exeter;
Cornwall; TR10 9EZ;
UK

ABSTRACT

It is well known that multijunction based concentration solar cells produced highest possible electric conversion efficiency. Moreover, these modern photovoltaic (PV) cells can be operated at a relatively high temperature with reasonable system efficiency. However, at very high operating temperatures, the power coefficient of the solar cells becomes negative. This paper presents a heat transfer model, which predicts the solar cell temperature for multijunction concentrating solar cell systems. This work models solar cells made of GaInP, GaAs and Ge with active aluminum back plates and anti-reflected glass plates. Air-active cooling was used to alleviate the operating solar cell temperature. Air is forced to flow within the ducts behind the solar cell assembly, and a finite difference technique has been used to solve the governing equations. The effects of the controlling parameters on solar cell temperatures are illustrated. Results show that the interaction of surface radiation and air convection can adequately cool the solar cell at medium concentration ratios. In addition, the ultimate values of the concentration ratio at which PV solar cells can be operated with reasonable efficiency have been obtained.

## 1.INTRODUCTION

The energy world's growing demands are expected to be filled by photovoltaics (PV), which directly convert solar energy into electricity. The conversion efficiency of modern multijunction cells has recently reached 44%. However, it has been found that the efficiency decreases with an increase in the operating temperature of solar cells [1]. On the contrary, the operating cell temperature increases remarkably with an increase in the concentration ratio, reaching well over 1200$^{o}$C at 400 suns [2]. Consequently, at high values of concentration ratio, solar cells need to be cooled during operation. Passive cooling is the efficient method for removing heat from high illumination photovoltaic cells. However, passive cooling rejects heat energy (approximately 60-90% of the total energy) to the environment as waste energy. Thus, active cooling systems enhance the overall efficiency and economic feasibility. Water is the favorable option for actively cooling the solar cells because of its high heat capacity. However, in some situations water is limited, so air becomes the preferred option, especially with the modern PV cells that can be operated up to 240°C while maintaining reasonable electric conversion efficiency [3, 4]. Cui Min et al. [2] and Octal and Frost [5] developed a theoretical thermal model to predict the temperature of the multijunction solar cell based on passive cooling systems. Vicenza et al. [6,7] used a silicon wafer with microchannels circulating water directly underneath the cells in an active cooling system.

Recently, Al-Amri and Tapas Mallick [8] developed a numerical heat transfer model for a triple junction concentrating solar cell system to predict the maximum cell temperature cooling actively by water-forced convection. It was found that the maximum cell temperature was strongly dependent on the flow rate and channel width.

The present paper has developed and presents an in-house developed thermal model for air active cooling of

concentrator triple junction solar cells with the presence of surface radiation.

## 2.CONCENTRATOR TRIPLE JUNCTION CELL ASSEMBLY DESIGN:

Figure 1 shows the schematic of the system geometry, which consists of a triple junction GaInP/GaAs/Ge solar cell, a Cu-Ag-Hg front contact to the solar cell, a 2 mm cover glass and a 1.5 mm thick aluminum back plate. The solar cell is attached to the cover glass and rear aluminum plate via an adhesive material. Forcing air to flow within the ducts behind the back plate and transferring some of the heat from the aluminum back plate to the opposite duct wall by surface radiation reduces the cell temperature. The two walls of the duct are assumed to be gray, opaque, and diffuse.

## 3.GOVERNING EQUATIONS AND BOUNDARY CONDITIONS:

The governing equations, which describe the physical situation depicted in Figure 1, are the energy conservation equations in the multi walls, the equations of continuity, momentum, energy conservation in the fluid, and the radiation constraint equations along each of the two duct surfaces. Under the usual boundary layer assumptions, neglecting the axial conduction of heat in both the solid and fluid region, the corresponding dimensionless equations that govern the conjugate laminar forced flow and the heat transfer in the entry-region of two parallel plates are:

$$\frac{\partial V}{\partial Y}+\frac{\partial U}{\partial Z}=0 \tag{1}$$

$$V\frac{\partial U}{\partial Y}+U\frac{\partial U}{\partial Z}=\quad\frac{dP}{dZ}+\frac{\partial^2 U}{\partial Y^2} \tag{2}$$

$$V\frac{\partial \theta_f}{\partial Y}+U\frac{\partial \theta_f}{\partial Z}=\frac{1}{Pr}\quad\frac{\partial^2 \theta_f}{\partial Y^2} \tag{3}$$

$$\frac{\partial^2 \theta_s}{\partial Y^2}=0 \tag{4}$$

The integral form of the continuity equation (1) is

$$F=\int_0^1 U dY=1 \tag{5}$$

The radiation constraint equations are

Surface 1 (Y=0)

$$N_{rad}\ \theta_\infty^4\left[\frac{1}{2}-\left(\frac{Z\,Re}{2}\right)\left(1+Z^2\,Re^2\right)^{-\frac{1}{2}}\right]$$

$$+\ N_{rad}\theta_e^4\left[\frac{1}{2}-\left(\frac{(L-Z)Re}{2}\right)\left(1+(L-Z)^2\,Re^2\right)^{-\frac{1}{2}}\right]$$

$$+\int_0^L\left\{\frac{1-\varepsilon_2}{\varepsilon_2}\left(\left.\frac{\partial\theta_f}{\partial Y}\right|_{Y=1^-}-\left.\frac{\partial\theta_s}{\partial Y}\right|_{Y=1^+}\right)+N_{rad}\theta_{w2}^4(Z)\right\}$$

$$*\frac{1}{2}\left[1+Re^2(Z-Z')^2\right]^{(-3/2)}RedZ'=$$

$$\frac{1-\varepsilon_1}{\varepsilon_1}\left[-\left.\frac{\partial\theta_f}{\partial Y}\right|_{Y=0^+}\right]$$

$$+\ N_{rad}\ \theta_{w_1}^4(Z)-\left.\frac{\partial\theta_f}{\partial Y}\right|_{Y=0+} \tag{6}$$

Where: $N_{rad}=\sigma q_1^3\frac{b^4}{k_f^4}$

Surface 2 (Y=1)

$$KR_{s_1-f}\left.\frac{\partial\theta_s}{\partial Y}\right|_{Y=1^+}+N_{rad}\ \theta_\infty^4\left[\frac{1}{2}-\left(\frac{Z\,Re}{2}\right)\left(1+Z^2\,Re^2\right)^{-\frac{1}{2}}\right]$$

$$+\ N_{rad}\ \theta_e^4\left[\frac{1}{2}-\left(\frac{(L-Z)}{2}Re\right)\left(1+(L-Z)^2\,Re^2\right)^{-\frac{1}{2}}\right]$$

$$+\int_0^L\left\{\frac{1-\varepsilon_1}{\varepsilon_1}\left(-\left.\frac{\partial\theta}{\partial Y}\right|_{Y=0^+}\right)+N_{rad}\theta_{w1}^4(Z)\right\}$$

$$*\frac{1}{2}\left[1+\mathrm{Re}^2(Z-Z')^2\right]^{(-3/2)}\mathrm{Re}dZ' =$$

$$\frac{1-\varepsilon_2}{\varepsilon_2}\left[\frac{\partial\theta_f}{\partial Y}\bigg|_{Y=1^-} - \frac{\partial\theta_s}{\partial Y}\bigg|_{Y=1^+}\right]$$

$$N_{rad}\,\theta_{w_2}^4(Z) - \frac{\partial\theta_f}{\partial Y}\bigg|_{Y=1^-} \qquad (7)$$

The conjugate convection field equations are subject to the following dimensionless boundary conditions:

For Z = 0 and $0 < Y < 1$

$$U = 1,\ V = P = \theta_f = 0 \qquad (8a)$$

For Z > 0 and Y = 0

$$U = V = 0 \qquad (8b)$$

For Z > 0 and $Y = Y_{S_{(i)-(i+1)}}$, i = 1 and 2

$$\frac{\partial\theta_s}{\partial Y}\bigg|_{Y=Y^-_{S_{(i)-(i+1)}}} = kR_{S_{(i+1)-(i)}}\ \frac{\partial\theta_s}{\partial Y}\bigg|_{Y=Y^+_{S_{(i)-(i+1)}}} \qquad (8d)$$

For $Y = Y_{S_{(i)-(i+1)}}$ and

$0 < Z < Z_c$ or $(Z_c+L_c) < Z < L$, i = 3 and 4

$$\frac{\partial\theta_s}{\partial Y}\bigg|_{Y=Y^-_{S_{(i)-(i+1)}}} = kR_{S_{(i+1)-(i)}}\ \frac{\partial\theta_s}{\partial Y}\bigg|_{Y=Y^+_{S_{(i)-(i+1)}}} + \frac{(1-\eta)\,\alpha_{s_i}(1-\alpha_g-\alpha_{ad})}{KR_{if}} \qquad (8e)$$

For $Y = Y_{S_{5-7}}$ and

$0 < Z < Z_c$ or $(Z_c+L_c) < Z < L$

$$\frac{\partial\theta_s}{\partial Y}\bigg|_{Y=Y^-_{S-7}} = kR_{S_{7-5}}\ \frac{\partial\theta_s}{\partial Y}\bigg|_{Y=Y^+_{S_{5-7}}} + \frac{(1-\eta)\,\alpha_{s_5}(1-\alpha_g-\alpha_{ad})}{KR_{5f}} \qquad (8f)$$

For $Y = Y_{S_{(i)-(i+1)}}$ and

$Z_c \le Z \le (Z_c + L_c)$, i = 3, 4, and 5

$$\frac{\partial\theta}{\partial Y}\bigg|_{Y=Y^-_{S_{(i)-(i+1)}}} = kR_{S_{(i+1)-(i)}}\ \frac{\partial\theta}{\partial Y}\bigg|_{Y=Y^+_{S_{(i)-(i+1)}}} \qquad (8g)$$

For $Y = Y_{S_{6-7}}$ and $Z_c \le Z \le (Z_c + L_c)$

$$\frac{\partial\theta}{\partial Y}\bigg|_{Y=Y^-_{S_{6-7}}} = kR_{S_{7-6}}\ \frac{\partial\theta}{\partial Y}\bigg|_{Y=Y^+_{S_{6-7}}} + \frac{\alpha_{s_6}(1-\alpha_g-\alpha_{ad})}{kR_{if}} \qquad (8h)$$

For Z > 0 and $Y = Y_{S_{7-8}}$

$$\frac{\partial\theta}{\partial Y}\bigg|_{Y=Y^-_{S_{7-8}}} = kR_{S_{8-7}}\ \frac{\partial\theta}{\partial Y}\bigg|_{Y=Y^+_{S_{7-8}}} + \frac{\alpha_{s_7}(1-\alpha_g-\alpha_{ad})}{kR_{if}} \qquad (8i)$$

For Z > 0 and $Y = Y_{S_8}$

$$\frac{\partial\theta}{\partial Y}\bigg|_{Y=Y_{S_8}} = \frac{\alpha_g}{kR_{8f}} \qquad (8j)$$

Where $kR_{if} = \frac{k_{s_i}}{k_{s_{i-1}}} * \frac{k_{s_{i-1}}}{k_{s_{i-2}}} * \ldots\ldots * \frac{k_{s_1}}{k_f}$,

$kR_{s_{(i+1)-i}} = \frac{k_{s_{i+1}}}{k_{s_i}}$, and $kR_{s_1-f} = \frac{k_{s_1}}{k_f}$

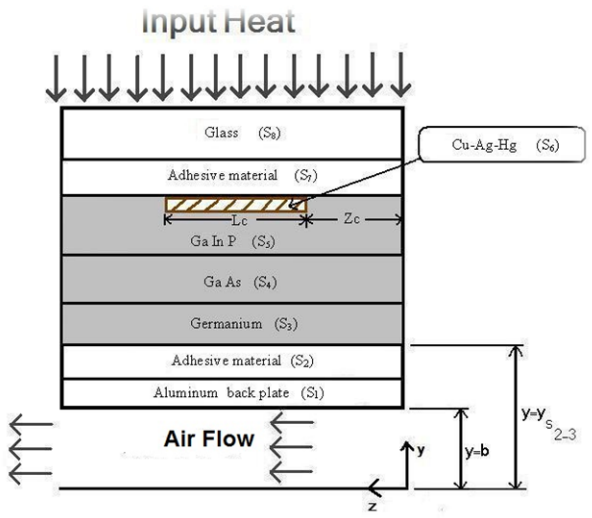


Figure .1: Schematic of the system geometry

Table.1: Thermophysical properties assumed in the simulation

| Component | Material | Length (mm) | Thickness (mm) | Thermal conductivity w/m.k | Absorptivity |
|---|---|---|---|---|---|
| Solar cell | GuInp | 10 | 0.1 | 73 | 0.04 |
| | GuAs | 10 | 0.2 | 65 | 0.4 |
| | Ge | 10 | 0.2 | 60 | 0.5 |
| Front contact | Cu+Ag +Hg | 2 | 0.025 | 300 | 0.15 |
| Glass cover | Low-iron glass | 10 | 2 | 12 | 0.04 |
| Adhesive | | 10 | 0.5 | 50 | 0.02 |
| Back plate | Aluminum | 10 | 1.5 | 238 | |

4.RESULTS AND DISCUSSION:

The governing equations (1) through (4) under the constraint of the integral continuity equation (5), and radiant constraint equations (6) and (7) and subject to the boundary conditions 8(a) – ( j ) are solved using a finite difference numerical technique. A mesh of 30,000 grid points was constructed and a Fortran program was written to model the problem. The system dimensions and thermophysical properties used in the simulation are summarized in Table 1. The temperature of air at channel entrance is assumed to be 27$^{o}$C and the efficiency of the triple junction solar cell is 0.38.

Figure 2 shows the variation of the maximum cell temperature with the duct wall emissivity for three selected values of concentration ratio: 100, 150, and 200. It can be observed from the figure that surface radiation has a significant effect on the maximum cell temperature. The surface radiation exchange between the two walls of the duct leads to transferring some of the heat from the aluminum back plate to the opposite duct wall, hence reducing the cell temperature. The higher the emissivity of the walls, the higher the effect of the surface radiation as shown in the figure. Thus, increasing the emissivity of the walls leads to operating the solar cell at a lower temperature and hence, an increase in cell efficiency. In addition, for a given value of operating temperature, as the emissivity of the walls increases, the solar cell can be operated at a higher concentration ratio without affecting its efficiency. In the present example pertinent to Figure 2, the solar cell operates at $240\,^{\circ}\mathrm{C}$ for concentration ratio=100 even though the two walls are excellent reflecting surfaces ($\varepsilon \approx 0$). On the contrary, for concentration ratio=200, the two walls should be excellent emitting surfaces ($\varepsilon \approx 1$) in order to operate the solar cell at $240\,^{\circ}\mathrm{C}$ as shown in the figure.

The recent PV cells can be operated up to $240\,^{\circ}\mathrm{C}$ with acceptable electric conversion efficiency [2,3]. Thus, in the present study, the concentration ratio at which PV cells operate at $240\,^{\circ}\mathrm{C}$ will hereinafter be referred to as the ultimate concentration ratio. Table 2 shows the ultimate values of the concentration ratio for some selected values of air inlet velocity and plate width at $\varepsilon = 1$. It is clear from the table that the ultimate value of the concentration ratio increases as the air velocity increases. In contrast, increasing plate width decreases the ultimate concentration ratio. This indicates that the operating solar cell temperature decreases with increasing air velocity or decreasing plate width for a given value of concentration ratio.

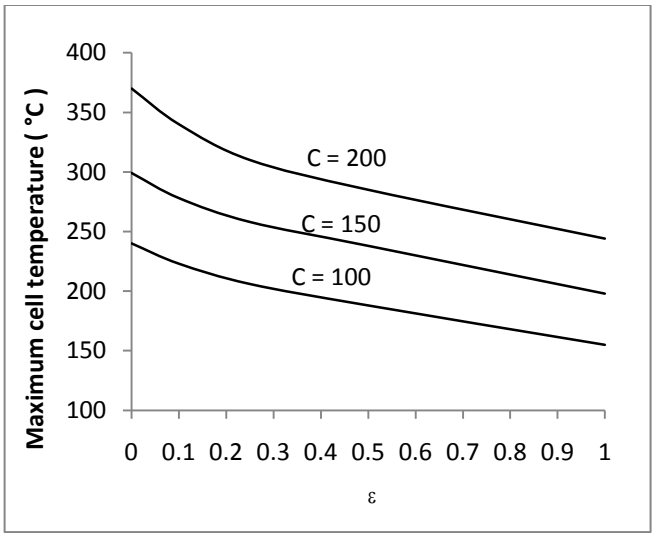


Figure.2: Maximum cell temperature under concentrated illumination for three selected values of emissivity: [ $u_\infty =$ 32 m/s].

Table.2: Ultimate values of concentration ratio for different values of inlet velocity and plate width at ε = 1.

| | $u_\infty = 8$ m/s | $u_\infty = 16$ m/s | $u_\infty = 32$ m/s |
|---|---|---|---|
| b=1mm | 130 | 158 | 198 |
| b=0.75mm | 170 | 201 | 254 |
| b=0.5mm | 257 | 290 | 345 |

## 5.CONCLUSIONS

The effect of surface emissivity of duct walls on the maximum triple junction solar cell temperature cooling actively by air-mixed convection has been studied numerically. It was found that the cell temperature can be reduced significantly by increasing surface emissivity. The ultimate values of the concentration ratio at which PV solar cells can be operated with reasonable efficiency are obtained for selected values of air inlet velocity and plate width.


## 6.ACKNOWLEDGEMENTS

This work was supported by King Abdulaziz City for Science and Technology, Saudi Arabia.


## 7.REFERENCES


(1) M.J. Huang, P.C. Eames, B. Norton, Thermal regulator of building-integrated photovoltaics using phase change materials, Int. J. Heat Mass Transfer 47 (2004) 2715-2733.

(2) Cui Min, Chen Nuofu, Yang Xiaoli, Wang Yu, Bai Yiming, and Zhang Xingwang, Thermal analysis and test for single concentrator solar cells, Journal of Semiconductors, Vol. 30, No. 4 (2009)

(3) D. Meneses-Rodriguez, PP. Horley, J. Gonzalez-Hernandez, YV. Vorobiev, PN. Gorley, Photovoltaic solar cells performance at elevated temperatures, Solar Energy 78 (2005) 243-250.

(4) K. Nishioka, T. Takamoto, T. Agui, M. Kaneiwa, Y. Uraoka, T. Fuyuki, Annual output estimation of concentrator photovoltaic systems using high-efficiency InGaP/InGaAs/Ge triple junction solar cells based on experimental solar cell's characteristics and field-test meteorological data, Solar Energy Mater Solar Cells 90 (2006) 57-67.

(5) H. Cotal and J. Frost, Heat transfer modeling of concentrator multijunction solar cell assemblies using finite difference techniques, 31st IEEE PVSC Conference ( 2010) 213-218.

(6) D. Vincenzi, F. Bizzi, M. Stefancich, C. Malagu, G. L. Morini, A. Antonini, G. Martinelli, Micromachined silicon heat exchanger for water cooling of concentrator solar cell, Conference record, PV in Europe Conference and Exhibition-From PV technology to Energy Solutions, Rome, Italy, 2002.

(7) Anja Royne, Christopher J. Dey, David R. Mills, Cooling of photovoltaic cells under concentrated illumination: A critical review, Solar Energy & Solar Cells 86 (2005) 451-483.

(8) F. Al-Amri and T.K. Mallick, Alleviating operating temperature of high concentration solar cell by active cooling, World Renewable Energy Forum (2012).


## 8.NOMENCLATURE

b channel spacing, m

C concentration ratio

$Gr^*$ modified Grashof number, $\frac{g\beta q_1 b^4}{\upsilon^2 K_f}$

K thermal conductivity, $W/m \cdot K$

$\ell$ plate length, m

L dimensionless plate length, = $\frac{\ell}{b\,Re}$

$N_{rad}$ radiation number, $\sigma q_1^3 b^4 / k_f^4$

Re Reynolds number, $= \frac{u_o b}{\upsilon}$

t solar cell assembly thickness, m

T temperature at any point, K

$T_\infty$ inlet temperature, K

$u_o$ entrance axial velocity, m/s

u longitudinal velocity component at any point, m/s

U dimensionless longitudinal velocity, $U=u/u_o$

v transverse velocity component at any point, m/s

V dimensionless transverse velocity, $V = b * v / \upsilon$

y horizontal coordinate, m

Y dimensionless horizontal coordinate, y / b

z vertical coordinate, m

Z dimensionless vertical coordinate, z / (b * Re)

9.GREEK SYMBOLS

$\upsilon$ kinematic fluid viscosity

$\rho$ fluid density, $kg/m^3$

$\mu$ dynamic fluid viscosity, $kg/m \cdot s$

$\alpha$ absorptivity

$\eta$ efficiency of the solar cell

$\theta$ dimensionless temperature at any point $\left[ = \frac{k_f T}{q_1 b} \right]$

$\theta_f$ dimensionless inlet temperature at any point $\left[ = \frac{k_f T_\infty}{q_1 b} \right]$

$\varepsilon$ wall emissivity

$\sigma$ Stefan Boltzman constant = $5.67*10^{-8}$ $W/m^2$ $k^4$

10.SUBSCRIPTS

ad adhesive material

e exit

f fluid

g glass

s solid

w wall of the channel

1 duct wall at Y = 0

2 duct wall at Y = 1